OPTIMAL DESIGN OF HYDRAULIC CAPSULE PIPELINES TRANSPORTING SPHERICAL CAPSULES

Taimoor Asim[*1] and Rakesh Mishra[2]
[1,2] School of Computing & Engineering
University of Huddersfield, Queensgate, Huddersfield HD1 3DH, UK
[1]t.asim@hud.ac.uk, [2]r.mishra@hud.ac.uk
[*]Corresponding author. Tel: +44 1484 472323

1. Abstract

Scarcity of fossil fuels is affecting efficiency of established modes of cargo transport within transportation industry. Extensive research is being carried out on improving efficiency of existing modes of cargo transport, as well as to develop alternative means of transporting goods. One such alternative method can be through the use of energy contained within fluid flowing in pipelines in order to transfer goods from one place to another. The present study focuses on the use of advanced numerical modelling tools to simulate the flow within Hydraulic Capsule Pipelines (HCPs) transporting Spherical Capsules with an aim of developing design equations. Hydraulic Capsule Pipeline is the term which refers to the transport of goods in hollow containers, typically of spherical or cylindrical shapes, termed as capsules, being carried along the pipeline by water. HCPs are being used in mineral industries and have potential for use in Oil & Gas sector. A novel modelling technique has been employed to carry out the investigations under various geometric and flow conditions within HCPs. Both qualitative and quantitative flow analysis has been carried out on the flow of spherical shaped capsules in an HCP for both on-shore and off-shore applications. Furthermore, based on Least-Cost Principle, an optimisation methodology has been developed for the design of single stage HCPs. The input to the optimisation model is the solid throughput required from the system, and the outputs are the optimal diameter of the HCPs and the pumping requirements for the capsule transporting system.

Keywords: Computational Fluid Dynamics, Fluid-particle Dynamics, Modelling, simulation, Multiphase systems

2. Introduction

Pipelines are an integral part of various industries throughout the world. The development of pipelines can be broadly categorised into three generations:

- First Generation (Single Phase Flow Pipelines)
- Second Generation (Multi-phase Flow Pipelines)
- Capsule Pipelines (both Pneumatic and Hydraulic)

The third generation of pipelines comprises of the transportation of Capsules through pipelines. These capsules are hollow containers filled with minerals, ores, radioactive

[*] Corresponding Author
Tel.: +44 1484 472323

materials or even goods such as mail, jewellery etc. In some cases, the material that needs to be transported is itself given the shape of the capsule. This technique is very famous in the transportation of coal, and such pipelines are termed as Coal-Log Pipelines (CLP).[1] The shape of the capsule is normally cylindrical or spherical where wheels are usually attached to the cylindrical capsules to overcome the static friction between the capsules and the pipe wall because of a larger contact area as compared to spherical capsules. Dominique et al. have numerically studied the motion of deformable capsules as well. [2-4] The economic surveys that have been conducted by some companies and universities, have shown that the capsule transportation is more economical than conventional methods of transporting goods such as trucks, rails etc.[5]

Ellis et al. have conducted a number of experimental investigations on horizontal HCPs, transporting both equi-density and heavy-density spherical capsules.[6-8] The studies are focused on developing empirical expressions for capsule velocity within the pipeline. These studies have taken into account the flow of a single capsule of various capsule-to-pipe diameter ratios ($k = \frac{d}{D}$), and flow velocities. It has been shown that the velocity of a capsule is a function of all these geometric and flow parameters. Furthermore, the motion of heavy-density spherical capsules in the pipeline is predominantly rotational. The experimental data of Ellis has been used in the present study as an input for modelling both the equi-density and heavy-density spherical capsules in horizontal pipes. Similar studies have been carried out by Mathur et al.[9], Round et al.[10], Mishra et al.[11] and Newton et al.[12]. Ulusarslan however conducted experimental studies on the flow of less-density spherical capsule train within a horizontal HCP.[13] The capsules have been made from polypropylene, having specific gravity of 0.87 and k=0.8. Pressure drop has been calculated across the test section for average flow velocities of 0.2 to 1.6m/sec. It has been reported that increase in the flow velocity increases not only the capsule velocity, but also the pressure drop across the pipe. Furthermore, increase in the solid phase concentration within the pipe also increases the pressure drop because of more resistance to the flow. The experimental data shows that the increase in the pressure drop within the pipe increases with increase in flow velocity. At higher flow velocity this increase becomes almost exponential. The experimental data of Ulusarslan has been used in the present study for the benchmarking of CFD predictions for the pressure drop within a horizontal HCP.

Chow carried out extensive experimental investigations on the flow of equi-density spherical capsules in a vertical pipe, where the range of flow velocities is from 1m/sec to 4m/sec.[14] Various capsule-to-pipe diameter ratios have been considered. Capsule velocities and pressure drop across the pipe have been measured, and semi-empirical correlations have been developed for these flow conditions. Similarly, Latto et al. conducted experimental studies on the flow of heavy-density spherical capsules in vertical HCPs, keeping the range of various parameters the same as Chow has taken.[15] Semi-empirical expressions for the velocity of the capsules and the pressure drop across the pipe have been developed. Chow and Latto's experimental data regarding the velocity of spherical capsules in vertical pipes has been used in the present study as a boundary condition.

Ulusarslan extended the work on the flow of spherical capsule train in a horizontal pipe to elbows, and have developed expressions for the pressure drop across them.[16] There is very

limited amount of information available in the published literature about the flow of spherical capsules in pipe bends. The present study uses a novel technique called Discrete Phase Modelling (DPM) in order to artificially simulate the flow of spherical capsules in pipe bends, both horizontal and vertical. Using this method, capsule velocity has been recorded.

Polderman reported design rules for hydraulic capsule systems for both on-shore and off-shore applications.[17] The design rules are based on such variables as the pressure drop in the pipeline, Reynolds Number of capsules etc. A general indication towards parameters that might be used for an optimisation model has been given. However, no such optimisation model has been developed, which can be used for designing a pipeline transporting capsules. Morteza et al. developed an optimisation model for pipelines transporting capsules based on maximum pumping efficiency.[18] Prabhata has developed an optimisation model for sediment transport pipelines based on the least-cost principle.[19] The model assumes the value of the friction factor as the input to the model, strictly limiting its usefulness for commercial applications. Swamee has developed a model for the optimisation of equi-density cylindrical capsules in a hydraulic pipeline.[20] The model is based on least-cost principle. The input to the model is the solid throughput required from the system. The friction factors considered, however, are not representative of the capsule flow in the pipeline, and hence severely limit the practicality of the model. Agarwal et. al. has developed an optimisation model for multi-stage pipelines transporting capsules.[21] The model is based on the principle of least-cost and uses the solid throughput as the input to the model. The model developed is applicable for contacting spherical capsules only, occupying the complete length of the pipeline. Furthermore, this optimisation model used limited parameters for the analysis of HCPs, and considers homogeneous model for pressure drop prediction. The friction factor used for the model is an approximation of the Colebrook – White's equation for friction factor in a hydraulic pipeline,[22] severely limiting the utility of the model in terms of accurate representation of the pressure drop in the pipeline transporting capsules. Yongbai has developed an optimisation model for hydraulic pipelines based on saving energy sources.[23] The model, however, cannot be used for multi-phase flows. A novel HCP optimisation model has been developed in the present study based on Least-Cost Principle covering wide range of flow conditions after developing novel predictive models for design variables such as major and minor pressure losses as a function of solid throughput, number of capsules, pipe diameter etc..

3. Pressure drop considerations in HCPs

The pressure drop in a hydraulic pipeline transporting a fluid can be computed from Darcy Weisbach equation:[24]

$$\Delta P = f \frac{L}{D} \frac{1}{2} \rho V^2 \quad (1)$$

where ΔP is the pressure drop across the pipe, f is darcy's friction factor, L is the length of the pipe, D is the diameter of the pipe, ρ is the density of fluid and V is the flow velocity within the pipe. Darcy's equation can be extended to compute pressure drop within HCPs. This can be achieved by separating the pressure drop within the pipeline due to water alone, and due to capsules only. This can be expressed as:

$$\Delta P_m = k_1 f_w \frac{L}{D} \frac{k_2 \rho_w (1-c) k_3 V_{av}^2}{2} + k_4 f_c \frac{L}{D} \frac{k_5 \rho_w c k_6 V_{av}^2}{2} \quad (2)$$

where ΔP_m represents the presser drop across the pipe due to the mixture flow, ρ_w is the density of water, c is the concentration of the solid phase in the mixture, V_{av} is the average flow velocity and the constants k_1, k_2, k_3, k_4, k_5, k_6 are the coefficients which relate the friction factor, density and the velocity of both the water and the capsules respectively to that of the mixture. If the effect of the concentration of the solid phase c and the constants k_1, k_2, k_3, k_4, k_5, k_6 are represented in friction factor due to water alone (f_w) and friction factor due to capsules only (f_c) then the equation (2) can be simplified as:

$$f_w = f(c, k_1, k_2, k_3) \tag{3}$$

$$f_c = f(c, k_4, k_5, k_6) \tag{4}$$

Hence, the pressure drop in an HCP can be computed as:

$$\Delta P_m = f_w \frac{L}{D} \frac{\rho_w {V_{av}}^2}{2} + f_c \frac{L}{D} \frac{\rho_w {V_{av}}^2}{2} \tag{5}$$

Equation (5) is valid for the horizontal HCPs. This equation can be extended further to include the elevation effects as:

$$\Delta P_m = f_w \frac{L}{D} \frac{\rho_w {V_{av}}^2}{2} + f_c \frac{L}{D} \frac{\rho_w {V_{av}}^2}{2} + \rho_w g \Delta h \tag{6}$$

where g is the gravitational acceleration and Δh is the elevation of the vertical HCP. Hence, equations (5) and (6) represent the major loses in HCPs. In order to compute the minor loses within HCPs (both horizontal and vertical); the following expressions have been derived:

$$K_l = \frac{\Delta P}{\frac{1}{2}\rho V^2} \tag{7}$$

$$\Delta P_m = K_{lw} \frac{n\, \rho_w {V_{av}}^2}{2} + K_{lc} \frac{n\, \rho_w {V_{av}}^2}{2} \tag{8}$$

$$\Delta P_m = K_{lw} \frac{n\, \rho_w {V_{av}}^2}{2} + K_{lc} \frac{n\, \rho_w {V_{av}}^2}{2} + \rho_w g \Delta h \tag{9}$$

where K_{lw} represent the loss coefficient of the bend due to water, K_{lc} is the loss coefficient of the bend due to capsule and n is the number of bends attached to the pipeline. Hence, equations (8) and (9) include the minor losses within HCPs. All these coefficients (equations (3) and (4)) can be determined by experimental/numerical techniques. In the present study it has been done by numerically simulating the flow of spherical capsule/s in an HCP, and by using data available in the literature as boundary conditions, and for validation purposes.

4. Geometrical Configurations of HCP

The geometry of the pipe has been created using commercial CFD package ANSYS. The geometry of the pipe has been created in three separate steps. The first section is named as Inlet pipe, the middle pipe as Test section, and the third as Outlet pipe, as shown in figure 1. A 5m long Inlet pipe has been included in order to satisfy the condition for the flow development, as mentioned by Munson et al.[25] Similarly, a 1m long Outlet pipe has been extended from the Test section in order to fulfil numerical solver's requirements i.e. the boundaries of the flow domain should be far away from the Test section. The Test section used in the present study is similar to that of Ulusarslan et al. i.e. 1m length, 100mm diameter and the pipe walls are hydrodynamically smooth, which means that the absolute roughness constant (ε) of the pipe is zero.[26]

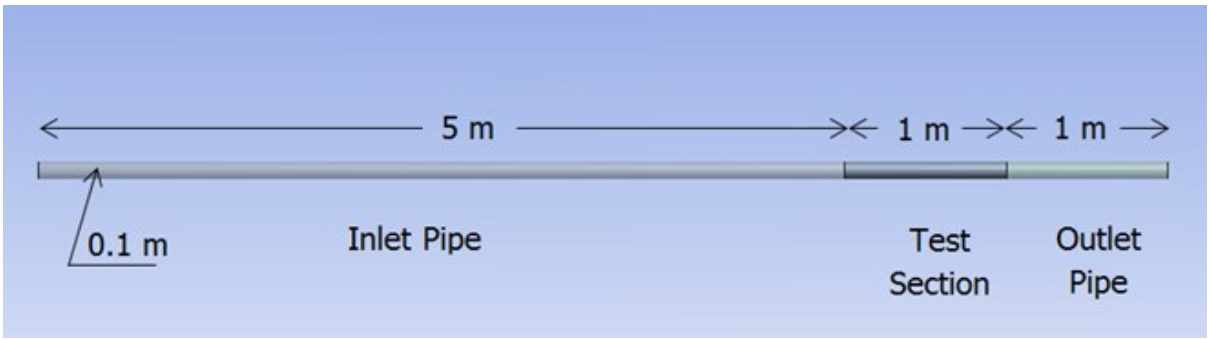

Figure 1. Geometry of the Pipe

Two different industrial scale pipe bend configurations, having R/r equal to 4 and 8, have been used in the present study, where R is the radius of the bend and r is the radius of the pipe. The geometric dimensions of the bends have been taken from industrial standards.[27] The angle of the bends under investigation is $\theta=90^{o}$. Figure 2 shows the different configurations of the bends being investigated.

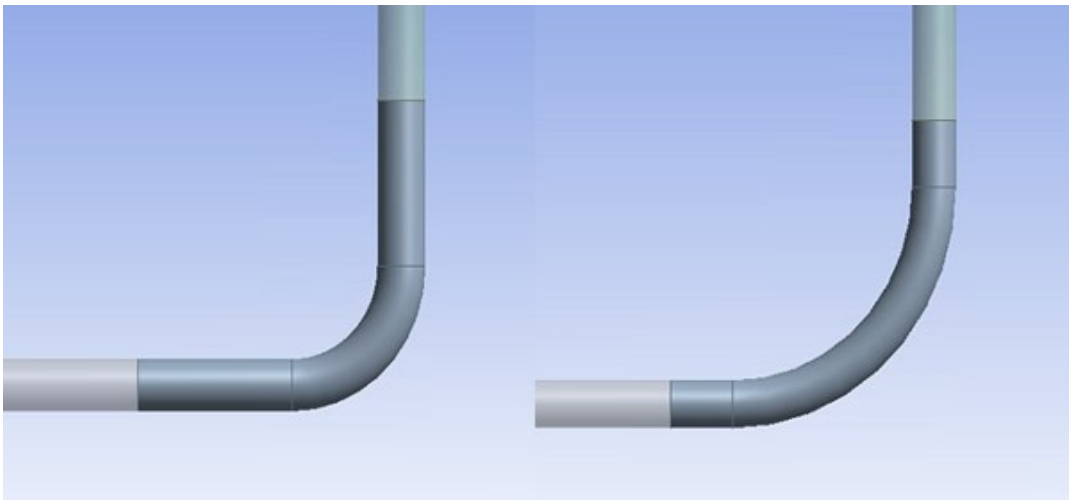

Figure 2. Geometry of the Bends

It is noteworthy here to mention the fact that the analyses presented in this study are based on the pressure drop considerations per unit length of the pipeline. In case of straight pipes, this is quite straightforward and is achieved by modelling the Test section having a length of 1m. For pipe bends, the volume of the bend has been calculated and compared against the volume of 1m of straight pipe. Additional pipe lengths have been added to the pipe bends, equally on both ends, in order to match the volumes of the two.

The spherical capsules have been introduced into the Test section of the pipe only. Various sizes and number of capsules have been used for the analysis of HCPs. Figure 3 shows the Test section of the pipe having three equi-density (density of capsules same as that of water) spherical capsules of k=0.5 with a spacing of 3d between them; d being the diameter of the capsules. It has been noticed by Ulusarslan et al. that there has been no significant change in the spacing between the capsules when velocity changes at a particular concentration. [26]

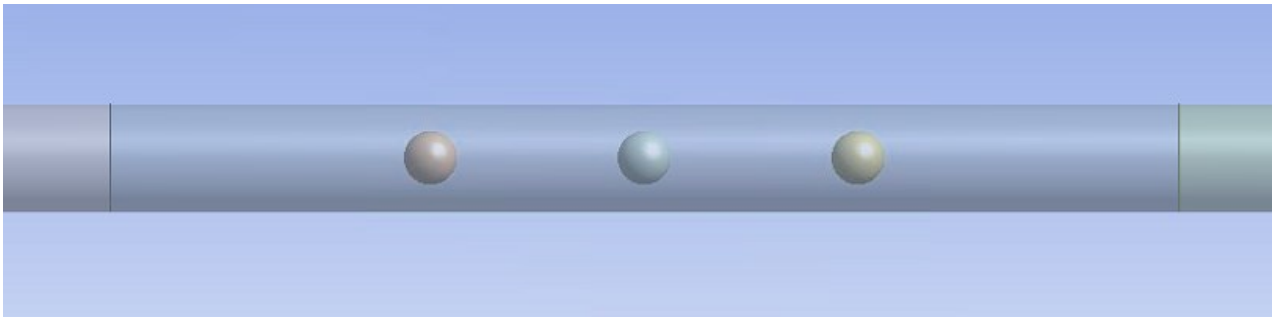

Figure 3. Geometry of Equi-Density Spherical Capsules

5. Discrete Phase Modelling of Capsules in Bends

The flow of capsules in a pipe bend is quite complicated to model as the trajectory of the capsules while passing through the bend cannot be known in advance. A novel modelling technique, called Discrete Phase Model (DPM), has been used in the present study to accommodate this. DPM solves transport equations for the continuous phase, i.e. water in case of hydraulic capsule bends. It also allows simulating a discrete second phase in a Lagrangian frame of reference.[28] This second phase consists of spherical particles (having same diameter as capsules) dispersed in the continuous phase. DPM computes the trajectories of these discrete phase entities. The coupling between the phases and its impact on both the discrete phase velocities and trajectories, and the continuous phase flow has been included in the present study. The discrete phase in the DPM is defined by defining the initial position and size of the capsules. These initial conditions, along with the inputs defining the physical properties of the discrete phase (capsule), are used to initiate trajectory and velocity calculations. The trajectory and velocity calculations are based on the force balance on the capsule. The trajectory of a discrete phase particle is predicted by integrating the force balance on the particle, which is written in a Lagrangian reference frame. This force balance equates the particle inertia with the forces acting on the particle, and can be written as:

$$\frac{dV_p}{dt} = F_D\,(V_w - V_P) + \frac{g\,(\rho_P - \rho_W)}{\rho_P} \tag{10}$$

where V_P and V_W are the velocities of particles and water respectively, ρ_P and ρ_W are the densities of particles and water respectively, t is time and g is the gravitational acceleration. $F_D(V_w\text{-}V_p)$ is the drag force per unit particle mass, and can be re-written as:

$$Drag\ Force = \frac{1}{2}\,\rho_w\left(V_w - V_p\right)^2 A\ C_d \tag{11}$$

where C_d is the drag coefficient and A is the cross-sectional area of the particle:

$$Drag\ Force = \frac{1}{2}\,Re_p\left(V_w - V_p\right)\frac{\pi d_p \mu}{4}\ C_d \tag{12}$$

where d_p is the particle diameter.

$$Drag\ Force\ per\ unit\ particle\ mass = \frac{\frac{1}{2}Re_p\left(V_w - V_p\right)\frac{\pi d_p \mu}{4} C_d}{\frac{\pi {d_p}^3}{6}\rho_p} \tag{13}$$

$$F_D = \frac{3\,\mu\,C_d\,Re_p}{4\,\rho_P\,{d_p}^2} \tag{14}$$

where C_D is the drag coefficient of the particles and Re_p is their Reynolds number. In the present study, Saffman's lift force due to shear has also been included in the study as an additional force acting on the particles.[29]

6. Meshing of the Flow Domain

The concept of hybrid meshing has been incorporated for the meshing of the flow domain. Two different meshes used i.e. a structured hexahedral mesh for the Inlet and Outlet pipes, while an unstructured tetrahedral mesh for the Test section due to the presence of capsule/s. Two different meshes with 1000,000 and 2000,000 mesh elements had been chosen for mesh independence testing. The results obtained, shown in table 1, depicts that the difference in the pressure drop across the HCP is less than 1% from the two meshes under consideration. It can therefore be concluded that the mesh with one million elements is capable of accurately predicting the flow features, and hence has been chosen for further analysis.

Table 1. Mesh Independence Results

Number of Mesh Elements	Pressure at Inlet	Pressure at Outlet	Pressure Drop per unit Length	Difference in Pressure Drops
	(Pa)	(Pa)	(Pa/m)	(%)
1 million	11163	401	10762	0.75
2 million	11265	584	10681	

It has been ensured that the y^+ value is under 10 for the capsules and the pipe wall, in order to resolve the boundary layer with reasonable accuracy. The y+ value has been computed as:

$$y^+ = \frac{\rho_W u_* y}{\mu_W} \tag{15}$$

where u_* is the friction velocity at the nearest wall and y is the nearest wall distance. The friction velocity has been computed as:

$$u_* = \sqrt{\frac{\tau_{Wall}}{\rho_W}} \tag{16}$$

where τ_{Wall} is the wall shear stress. Using equations (15) and (16), and computing wall shear stress from CFD predictions, and keeping y^+ under 10, y values have been computed, and have been specified as the first layer distance from the wall. The y values of 0.02mm and 0.03mm have been computed for the pipe wall and the capsule/s based on an average flow velocity of 4m/sec. At lower flow velocities, these values increase, however, in the present study, they have been kept constant to ensure reasonably accurate resolution of the boundary layer, both around the capsule/s and the pipe wall. The mesh of the flow domain is shown in figure 4.

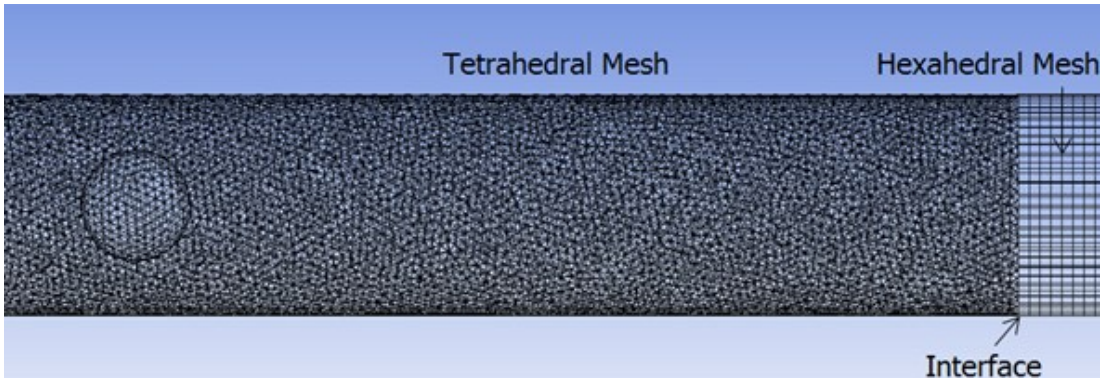

Figure 4. Meshing of the Flow Domain

7. Selection of the Physical Models

The velocity of the flow within HCPs is such that the compressibility effects can be neglected. Therefore, a pressure-based solver has been used for the analysis, keeping the density of water, and only computing the variations in the pressure within the pipeline. HCPs are considered to deliver a constant solid throughput, and hence, the flow is considered to be steady. A similar approach has been adopted by Khalil et. al.[30] Furthermore, in practical applications of HCPs, the velocity of the flow normally ranges from 0.5m/sec to 4m/sec, as discussed in the literature review.[6-9] These velocities correspond to Reynolds number of 50,000 to 400,000, hence, the flow is considered to be turbulent in such pipelines. As far as the transport of capsules in a pipeline is concerned, due to the formation of a wake region downstream of the capsules, and the flow separation phenomena, Shear Stress Transport (SST) k-ω model has been chosen for the modelling of turbulence. The primary reason behind choosing k-ω model is its superiority in accurately modelling the wake regions and extreme pressure gradients, which are expected to occur between the capsule/s and the pipe wall, i.e. the annulus region. Khalil et. al. has also shown that SST k-ω turbulence model predicts the changes in the flow parameters in HCPs with reasonable accuracy.

The SST-k-ω is a two equation model and includes the following refinements:

- The standard k-ω model and the transformed k-ε model are both multiplied by a blending function, and both models are added together. The blending function is designed to be one in the near-wall region, which activates the standard k-ω model, and zero away from the surface, which activates the transformed k-ε model.

- The definition of the turbulent viscosity is modified to account for the transport of the turbulent shear stress.

These features make the SST k-ω model more accurate and reliable for a wider class of flows such as adverse pressure gradient flows, aerofoils, transonic shock waves etc. Other modifications include the addition of a cross-diffusion term in the ω equation and a blending function to ensure that the model equations behave appropriately in both the near-wall and far-field zones, which makes this model most suitable for analysing HCPs.

8. Boundary Conditions

The boundary types and conditions that have been specified are listed in table 2.

Table 2. Boundary Conditions

Boundary Name	Boundary Type	Boundary Conditions
Inlet to the Pipe	Velocity Inlet	1 – 4m/sec
Outlet of the Pipe	Pressure Outlet	0Pa,g
Wall of the Pipe	Stationary Wall	No-Slip
Capsules	Translating/Rotating Walls in the direction of the flow	From Literature

8.1 Capsule Velocity in Horizontal HCPs

As discussed earlier, experimental data of Ellis has been used to develop semi-empirical expressions for the capsule holdup, where capsule holdup is defined as:[6]

$$H = \frac{V_c}{V_{av}} \tag{17}$$

where V_c is the capsule velocity and V_{av} is the average flow velocity. Equations (18) and (19) represent equi-density and heavy-density spherical capsules' velocities in horizontal HCPs respectively. Ellis observed that the heavy-density spherical capsules flow in the HCP predominantly by rotation, hence, for heavy-density spherical capsules, rotational velocity (ωc) has been computed and specified in the numerical simulations, alongwith the translational component (Vc), which is equal to (ωc * d/2). The velocities of the equi-density spherical capsule/s, calculated using equation (18), and obtained from the experimental data, have been plotted in figure 5. It can be clearly seen that the calculated velocities of the

capsule/s are in good agreement with the experimental data, and more than 90% of the data lies within ±5% error bound of equation (18).

$$Vc = (1.22 * Vav) - (0.15 * k * Vav) \tag{18}$$

$$\omega c = \frac{[(1.067 * Vav) - (0.0196 * s * Vav) + (0.042 * k * Vav)]}{\frac{d}{2}} \tag{19}$$

where s is the specific gravity of the capsule/s.

A 2inch flow loop based HCP test setup has been developed and the capsule velocities have been recorded for various flow velocities and capsule sizes. It has been observed that the experimentally recorded capsule velocities are in close agreement with the one calculated through the use of equations (18) and (19).

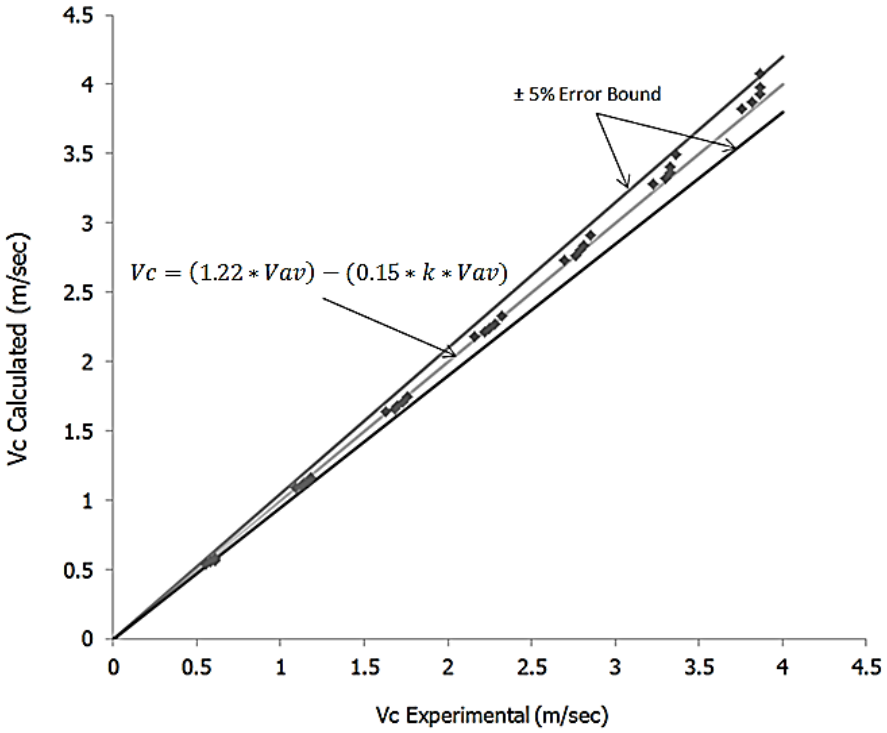

Figure 5. Difference between calculated and experimentally measured Vc

8.2 Capsule Velocity in Vertical HCPs

Chow has developed semi-empirical expressions for the capsule holdup in vertical HCPs.[14] These expressions have been used in the present study because the range of geometrical and flow parameters considered by Chow is the same as considered in the present study, thus, these expressions are valid for this study as well. Equations (20) and (21) represent the holdup for equi-density and heavy-density spherical capsules in vertical HCPs respectively.

$$\frac{Vc}{Vav} = \frac{1}{k^{0.34}} \tag{20}$$

$$\frac{Vc}{Vav} = \frac{1}{k^{0.34}} - \frac{Vav\left(\sqrt{\frac{\left(\frac{4}{3}gD(s-1)\right)}{k}}\left(1-k^2\right)\left(1-\frac{1}{s}\right)^{0.05}\right)}{k^{0.34}} \tag{21}$$

8.3 Capsule Velocity in Pipe Bends

As there is very limited amount of studies carried out on the flow of spherical capsule in pipe bends, Discrete Phase Modelling has been used in the present study in order to predict the velocity of capsule/s. However, an assumption has been made that only one capsule passes through the bend at a particular time. This assumption has been made in order to facilitate the numerical process. As the effective length of the pipe fittings, such as pipe bends, in any on-shore/off-shore pipeline system is negligibly small as compared to the length of straight pipes in the system, this assumption yields reasonably accurate results. Furthermore, the velocity of a capsule depends on its angular position within the bend. Hence, the analysis on the flow of spherical capsules in a pipe bend has been carried out at six equally spaced angular positions of 0^O, 18^O, 36^O, 54^O, 72^O and 90^O to cover a wide range of analysis. After conducting some preliminary investigations, it has been observed that the pressure drop in a pipe bend transporting spherical capsules is independent of the angular position of the capsule, where the density of the capsules is equal to that of water. However, the pressure drop is different at different locations in case of the flow of heavy-density spherical capsules in pipe bends. Hence, an average pressure drop has been considered for the analysis of the flow of heavy-density capsules in pipe bends. The average percentage error in pressure drop estimation is less than 5%.

9. Solver Settings

Application based solver settings are required to accurately predict the fluid flow behaviour in the flow domain. These settings comprise:

- Pressure – Velocity Coupling
- Gradient
- Spatial Discretisation

The Navier-Stokes equations are solved in discretised form. This refers to linear dependency of velocity on pressure and vice versa. Hence, a pressure–velocity is required to predict the pressure distribution in the flow domain with reasonable accuracy. In the present study, SIMPLE algorithm for pressure–velocity coupling has been incorporated because it converges the solution faster and is often quite accurate for flows in and around simple geometries such as spheres, cylinders etc.[31] In SIMPLE algorithm, approximation of the velocity field is obtained by solving the momentum equation. The pressure gradient term is calculated using the pressure distribution from the previous iteration or an initial guess. The pressure equation

is formulated and solved in order to obtain the new pressure distribution. Velocities are corrected and a new set of conservative fluxes is calculated.

Gradients are needed for constructing values of a scalar at the cell faces, for computing secondary diffusion terms and velocity derivatives. Green–Gauss Node–based gradient evaluation has been used in the present study.[32] This scheme reconstructs exact values of a linear function at a node from surrounding cell–centred values on arbitrary unstructured meshes by solving a constrained minimization problem, preserving a second-order spatial accuracy.

The CFD solver stores discrete values of the scalars at the cell centres. However, face values are required for the convection terms and must be interpolated from the cell centre values. This is accomplished using an upwind spatial discretisation scheme. Upwinding means that the face value is derived from quantities in the cell upstream, or upwind relative to the direction of the normal velocity. In the present study, 2^{nd} order upwind schemes have been chosen for pressure, momentum, turbulent kinetic energy and turbulent dissipation rate. The use of 2^{nd} order upwind scheme results in increased accuracy of the results obtained.[33]

10. Scope of Numerical Investigations

Full Factorial Design of Experiments (DoE) has been used in the present study in order to find out the required number of numerical simulations for the accurate prediction of pressure drop within HCPs. Minitab 17 Statistical Software has been used for this purpose. The factors considered for the flow spherical capsules in HCPs, and their levels, are presented in table 3.

Table 3. Factors and Levels for Full Factorial Design of an HCP

Factor	Level 1	Level 2	Level 3	Level 4
Number of Capsules in the train (N/L)	1	2	3	N/A
k	0.5	0.7	0.9	N/A
V_{av}	1	2	3	4
Spacing between the capsules (Sc)	1d	3d	5d	N/A
R/r	4	8	N/A	N/A
s	1	2.7	N/A	N/A

The resulting numbers of numerical experiments, which are equal to 369, have been performed, and the pressure drop per unit length of the pipeline has been recorded for each simulation. Semi-empirical expressions, similar to equations (5-6 and 8-9), have then been developed. These semi-empirical expressions have then been used to develop an optimisation method, based on Least Cost Principle, for HCPs transporting spherical capsules.

11. Benchmark Tests

One of the most important steps while conducting numerical studies is the benchmarking of the results. This means that some of the results obtained from the numerical simulations are compared against experimental results to have confidence on practical viability of these simulations. Hence, all the geometric, flow and solver-related parameters/variables become important in benchmarking studies. In the present study, the numerical model has been validated against the experimental findings for the pressure drop in the pipeline given by Ulusarslan.[34] The numerical model has been set for the conditions listed in table 4, in addition to the one already discussed regarding the geometry of the pipe, which is in accordance with the test apparatus of Ulusarslan.[35]

Table 4. Validation Tests

Name / Property	Value / Range / Comment	Units
Specific Gravity	0.87	N/A
k	0.8	N/A
Vav	0.2 – 1	(m/sec)
Capsule Shape	Spherical	N/A
Number of Capsules	Depending on concentration	N/A

Further to the aforementioned discussion, and after numerically solving the cases discussed in table 4, figure 6 depicts the variations in the pressure drop within the pipeline, from both CFD and experiments, at various flow velocities, for the flow of equi-density spherical capsules in a horizontal pipeline. It can be seen that the CFD results are in close agreement with the experimental results, with an average variation of less than 5%. It can be thus concluded that the numerical model considered in the present study does represent the physical model of a pipeline transporting capsules.

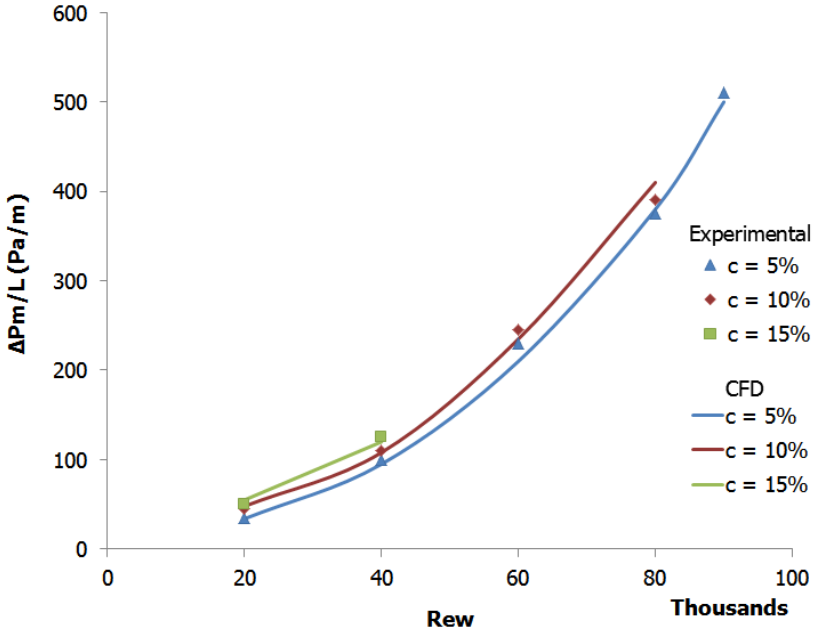

Figure 6. Validation of the CFD results with respect to the Experimental results

12. Results and Discussion

Local flow field analysis for the flow of spherical capsules in a hydraulic capsule pipeline has been documented here. The main focus of these analyses is to link the local flow features with the global flow parameters like the pressure drop. The effects of several geometrical and flow conditions on the local flow features have been obtained numerically. These are the effects of the capsule concentration within the HCP, capsule size, average flow velocity, and specific gravity of the capsules, along-with the effects of pipe inclination and pipe curvature.

Figure 7 depicts the variations in the static gauge pressure distribution within the test section of the horizontal pipe transporting a single equi-density spherical capsule of k=0.5 at V_{av}=1m/sec. It can be seen that the presence of a capsule makes the static gauge pressure distribution highly non-uniform inside the pipe altogether as compared to single phase flow where it is known that static pressure almost remains constant at a pipe cross section.[36] The pressure gradients in the vicinity of the capsule are large, as can be seen at upstream and downstream sections of the capsule. At the upstream of the capsule, the static gauge pressure increases to 738Pa as the fluid approaches the capsule. This happens due to the additional resistance offered by the capsule to the flow within the pipe because different flow velocities of flowing fluid and capsule. The flow then passes through the annulus between the pipe wall and the capsule. As the cross sectional area decreases the pressure decreases to -137Pa. Once the flow exits the annulus, due to the increase in the cross-sectional area, the static gauge pressure of water recovers to some extent. It can be seen in the figure that the static gauge pressure downstream has been recovered to 130Pa, as compared to 181Pa at far upstream location.

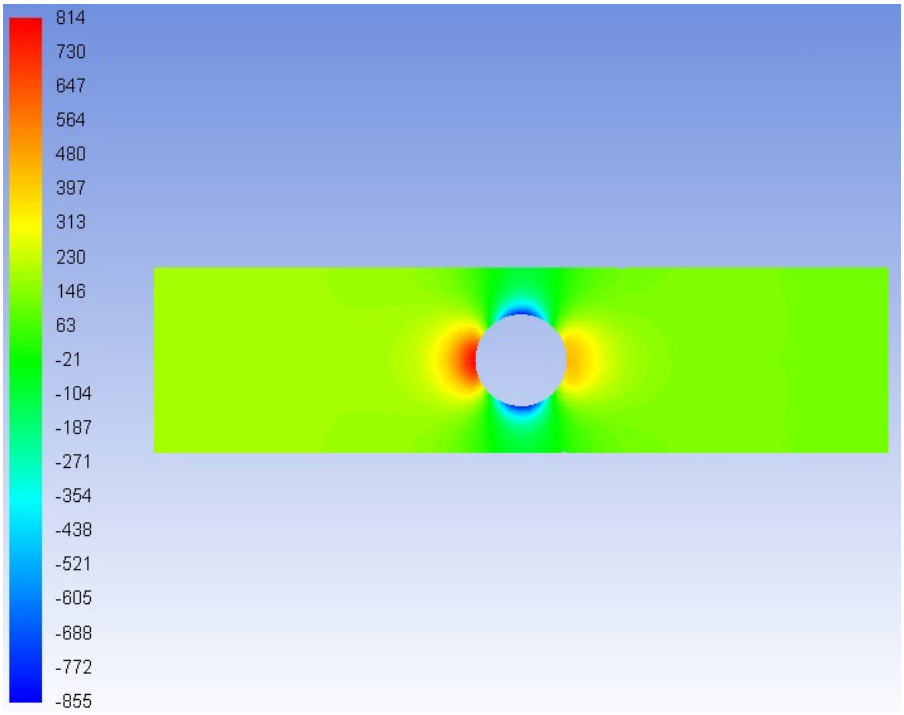

Figure 7. Variations in Static Gauge Pressure for a Single Equi-Density Spherical Capsule of k=0.5 in a Horizontal Pipe at V_{av}=1m/sec

12.1 Effect of Capsule Concentration

Figure 8 depicts the static gauge pressure variations in a horizontal hydraulic pipe carrying three equi-density spherical capsules of k=0.5 at V_{av}=1m/sec. The spacing between the capsules is equal to one diameter of the capsule. The trend of the static gauge pressure distribution is the same as observed for a single spherical capsule. The pressure at upstream location has increased to 248Pa (27%) while it has decreased to 117Pa (11%) downstream as compared to a single spherical capsule. An overall static gauge pressure drop increase of 16% has been observed for N/L=3 as compared to N/L=1, where N is the number of capsules within the test section of the pipeline, and L is the length of test section. Hence, N/L represents the concentration of capsules in the test section of the pipeline. It can be concluded that increasing the capsule concentration within the pipeline significantly increases the pressure drop across the pipeline.

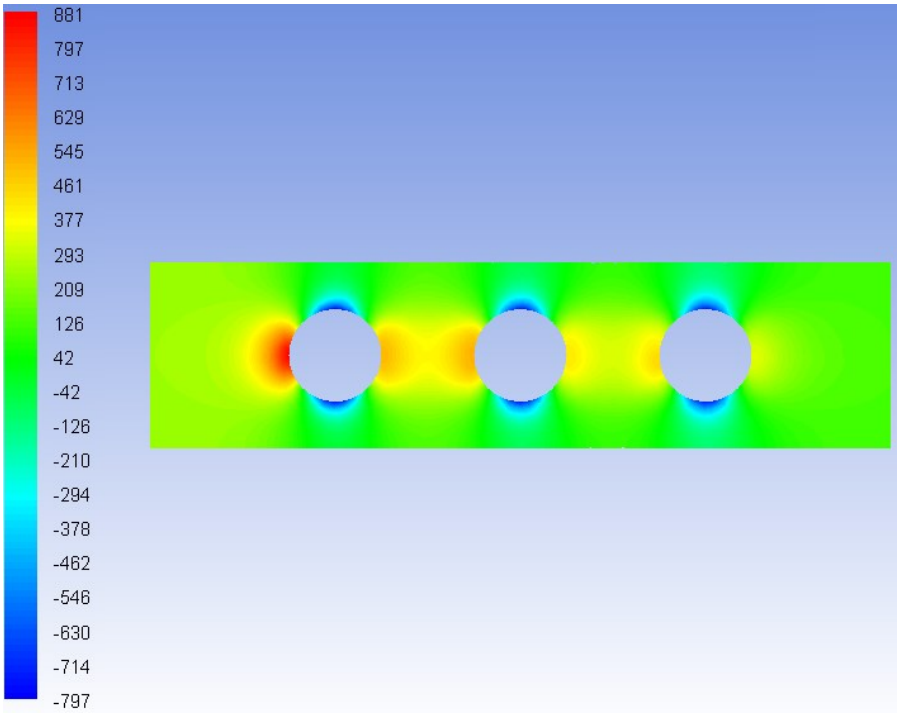

Figure 8. Variations in Static Gauge Pressure for three Equi-Density Spherical capsules of k=0.5, with 1d spacing between them, in a Horizontal Pipe at V_{av}=1m/sec

12.2 Effect of Capsule Spacing

Figure 9 depicts the static gauge pressure variations in a horizontal hydraulic pipe carrying three equi-density spherical capsules of k=0.5 at V_{av}=1m/sec. The spacing between the capsules is equal to five diameters of the capsule. The trend of the static gauge pressure distribution is the same as observed for Sc=1d. The pressure at upstream location has increased by 7% while it has decreased 14% downstream as compared to Sc=1d case. An overall pressure drop increase of 2% has been observed for Sc=5d as compared to Sc=1d. Hence, it can be concluded that increase in the spacing between the capsules, and keeping the concentration of the capsules within the pipeline constant, has negligibly small effect on the pressure drop across the pipeline.

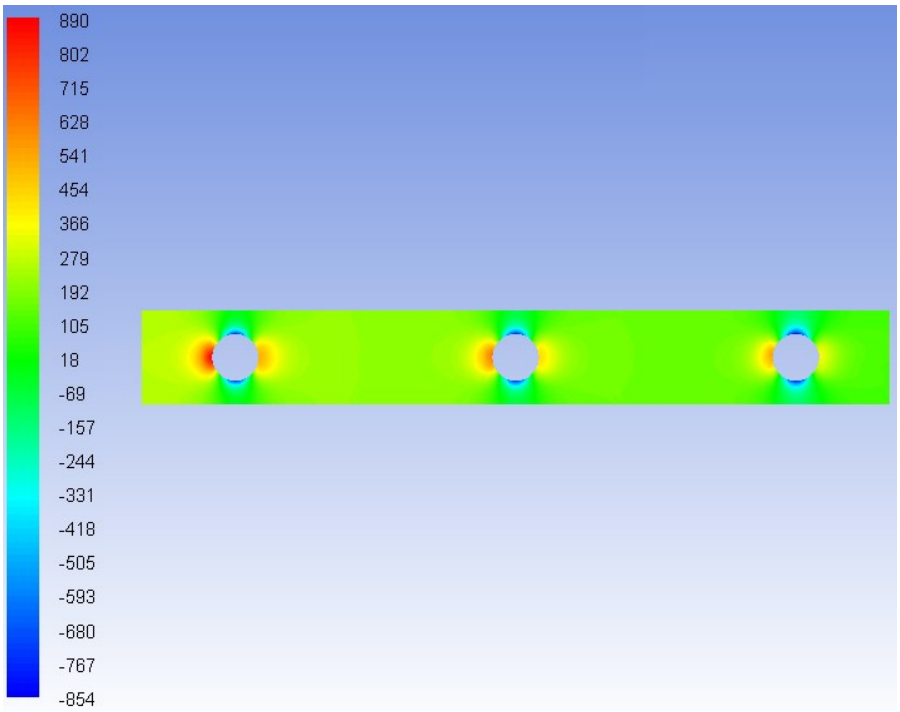

Figure 9. Variations in Static Gauge Pressure for three Equi-Density Spherical capsules of k=0.5, with 5d spacing between them, in a Horizontal Pipe at V_{av}=1m/sec

12.3 Effect of Capsule Size

Figure 10 shows the static gauge pressure distribution in an equi-density spherical capsule transporting horizontal pipe for k=0.9 and V_{av}=1m/sec. It can be seen that although the overall pressure distribution seems to be similar to the case with k=0.5 at the same average flow velocity, but the static gauge pressure at upstream location has increased by 88%, while the static gauge pressure at downstream location has decreased by 116%, which suggests that the overall pressure drop in the pipe has increased significantly. The pressure drop between the inlet and the outlet of the pipe is 1450Pa, which is 91.5% higher than the pressure drop for k=0.5. Furthermore, the static gauge pressure in the annulus region has decreased by 99%, while the static gauge pressure at the immediate upstream location of the capsule has increased by 58%. Such a sharp decrease in the static gauge pressure in the annulus region is due to the fact that the cross-sectional area of the flow has reduced by 80%. Hence, it can be concluded that increase in the size of capsule increases the pressure drop considerably.

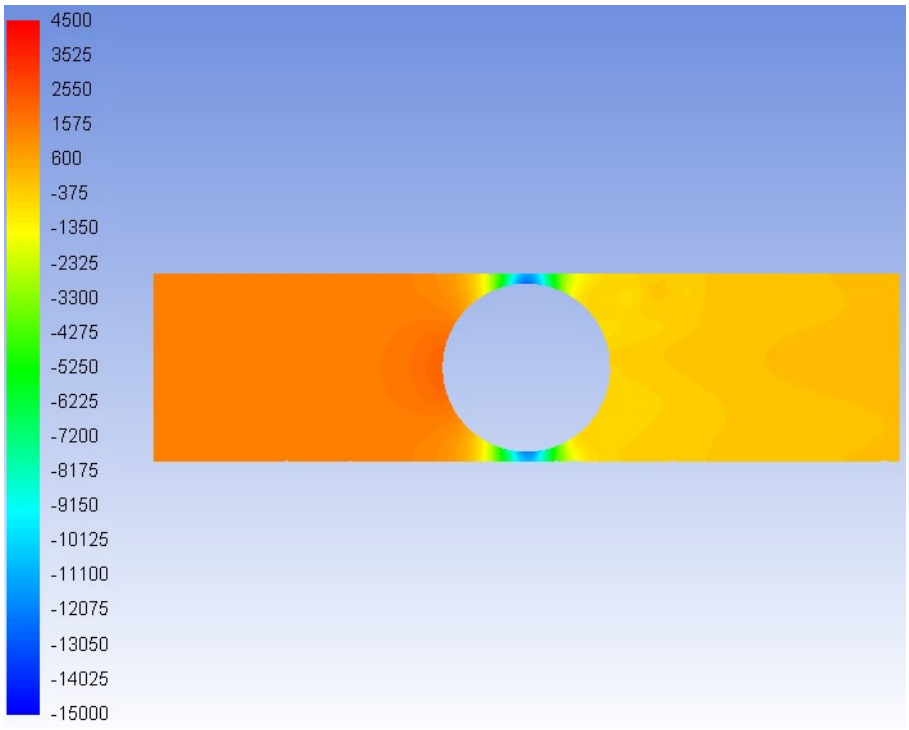

Figure 10. Variations in Static Gauge Pressure for a Single Equi-Density Spherical Capsule of k=0.9 in a Horizontal Pipe at V_{av}=1m/sec

12.4 Effect of Flow Velocity

To investigate the effect of the average flow velocity on the flow structure within the pipe, an average velocity of 4m/sec for an equi-density spherical capsule of k=0.5 has been chosen for analysis. Figure 11 depicts the static gauge pressure variations in a horizontal pipe for an average flow velocity of 4m/sec, keeping k=0.5. The trend of the static gauge pressure distribution is the same as observed for V_{av}=1m/sec i.e. a high static gauge pressure of 2414Pa at the upstream location, a very low static gauge pressure of -2632Pa in the annulus region, a relatively low static gauge pressure of 1379Pa at downstream location as compared to upstream location, and a very high static gauge pressure of 10047Pa at the location where the flow strikes the capsule. There is an average increase of 92% in the static gauge pressure at the upstream, downstream and the point of highest pressure as compared to V_{av}=1m/sec. Furthermore, there is a decrease of 95% in the static gauge pressure in the annulus region. The pressure drop between the inlet and the outlet of the pipe is 1533Pa, which is 92% higher than the pressure drop for V_{av}=1m/sec. It can be concluded that increase in the average velocity of the flow increases the pressure drop, but does not affect the overall pressure distribution in a capsule transporting pipe. The same trend has been observed by Ulusarslan.[37] Hence, it can be concluded that increasing the average flow velocity within an HCP increases the pressure drop across it.

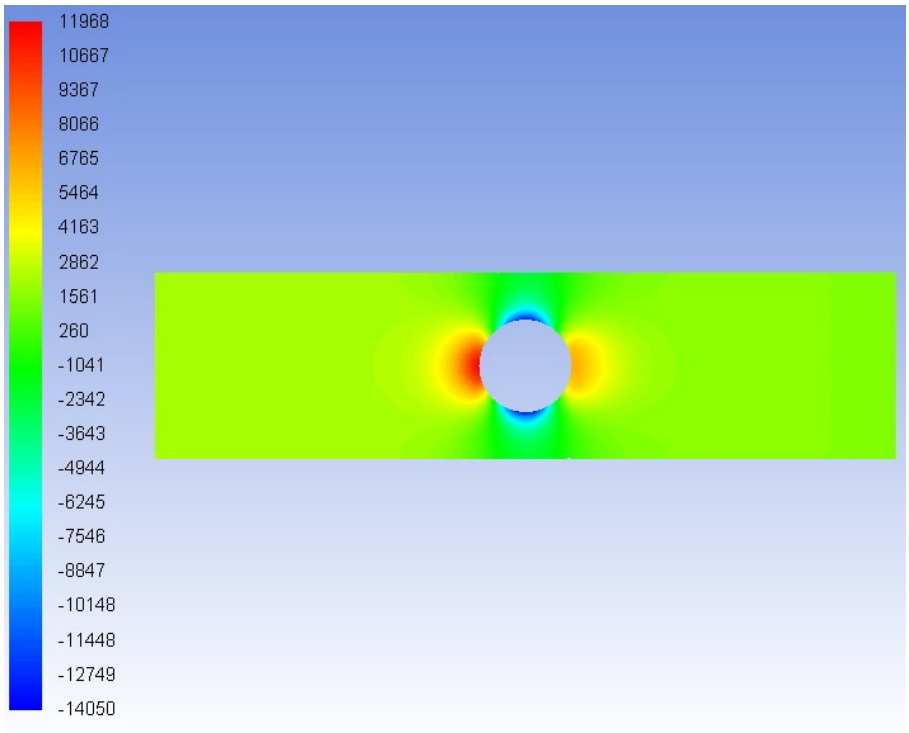

Figure 11. Variations in Static Gauge Pressure for a Single Equi-Density Spherical Capsule of k=0.5 in a Horizontal Pipe at V_{av}=4m/sec

12.5 Effect of Capsule Density

The flow of heavy-density spherical capsules in a horizontal pipe is different from the flow of equi-density capsules. The main reason for this is the weight of the heavy-density capsules, which becomes higher than the buoyant forces acting on the capsules. Thus, the capsules no longer remain concentric to the pipeline, and travel along the bottom wall of the pipe. The force needed to propel a concentric capsule is different to a capsule moving along the bottom wall of the pipeline because the flow structure in the two cases will be significantly different.

As far as the flow of spherical capsules in a horizontal pipeline is concerned, where the capsule density is not equal to the density of water, Teke has reported that the capsules only rotate at Reynolds number of $1.5x10^5$ and under.[38] At higher Reynolds numbers, the capsules tend to move towards the pipe axis, where the primary motion of the capsule is due to sliding/translation. This happens because of non-uniform pressure gradients acting on the upstream face of the capsules. However, the capsules considered by Teke were only slightly less dense than water. As the difference in the densities of the capsules and the carrying fluid increases, the weight of the capsules also increases. Higher average flow velocities will be required to overcome this force and to make the capsules water-borne.[7] As the heavy-density capsules considered in the present study are made of aluminum (s=2.7), under the realistic flow velocities in 4inch pipelines, it is expected, and has been observed in the flow loop tests, that the capsules travel along the bottom wall of the pipe.

Figure 12 depicts the variations in the static gauge pressure distribution within the test section of the horizontal pipe transporting a single equi-density spherical capsule of k=0.5 at

V_{av}=1m/sec. It can be seen that the presence of a heavy-density spherical capsule within the pipe changes the pressure distribution altogether as compared to an equi-density spherical capsule. The pressure gradients in the vicinity of the capsule are severely large as seen in the vicinity of the capsule. At upstream location, the static gauge pressure of water increases from 290Pa to 669Pa as it approaches the capsule. This happens due to the additional resistance offered by the capsule to the flow within the pipe, due to the generation of secondary flow features. The flow then passes through the annulus between the pipe wall and the capsule. As the cross-sectional area decreases, the static gauge pressure of water decreases to 45Pa. Once the flow exits the annulus, due to the increase in the cross-sectional area, the static gauge pressure recovers to some extent. It can be seen in the figure that the pressure downstream has been recovered to 117Pa, as compared to 290Pa at upstream location. Hence, it can be concluded that increasing the specific gravity of the capsule increases the pressure drop across the pipeline, where specific gravity of the capsule can be expressed as:

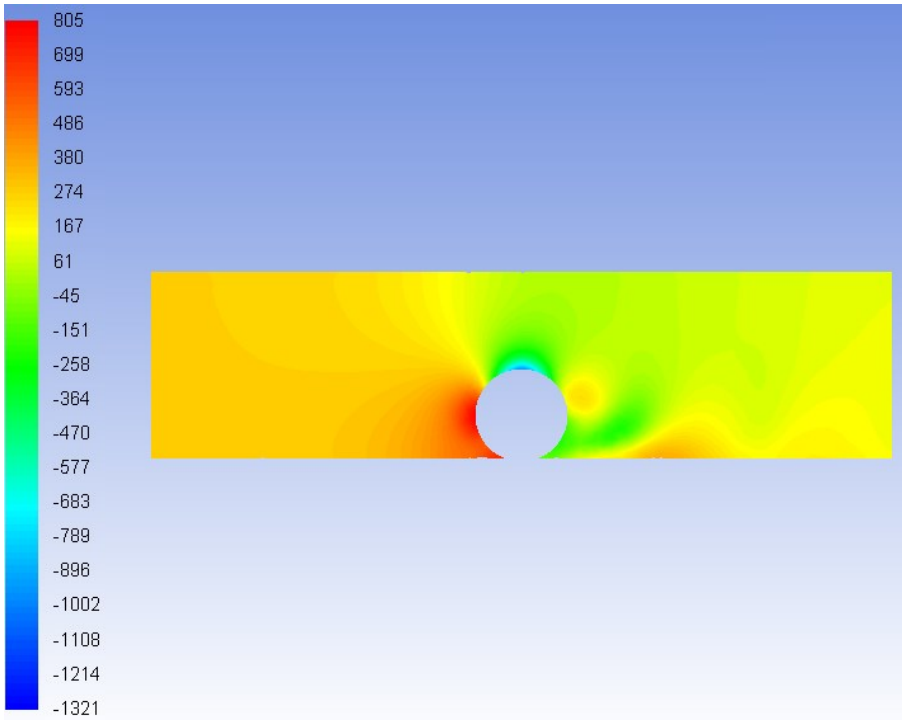

Figure 12. Variations in Static Gauge Pressure for a Single Heavy-Density Spherical Capsule of k=0.5 and s=2.7, in a Horizontal Pipe at V_{av}=1m/sec

$$s = \frac{\rho_c}{\rho_w} \tag{22}$$

where ρ_c and ρ_w are the densities of capsule and water respectively.

12.6 Effect of Pipe's Inclination

Figure 13 depicts the variations in the static gauge pressure distribution within the test section of the vertical pipe transporting a single equi-density spherical capsule of k=0.5 at V_{av}=1m/sec. It can be seen that the presence of a capsule changes the pressure distribution inside a vertical pipe. The static gauge pressure in the pipeline decreases continuously from

the inlet to the outlet of the pipe. It can be seen that the pressure decreases by 15% upstream of the capsule and 28% downstream of the capsule. At such a low velocity of the capsule in a vertical pipe, the effect of the presence of the capsule on the pressure drop within the pipeline is dominated by the pressure drop due to the elevation of the pipe.

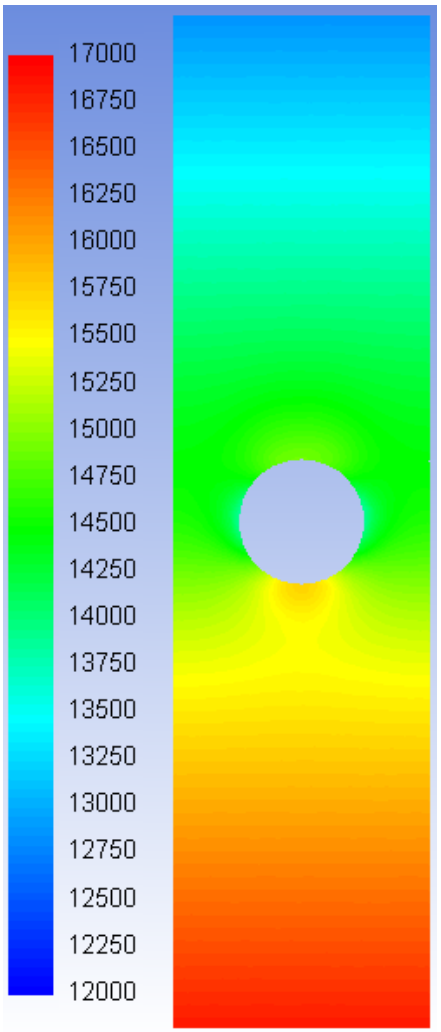

Figure 13. Variations in Static Gauge Pressure for a Single Equi-Density Spherical Capsule of k=0.5 in a Vertical Pipe at V_{av}=1m/sec

In comparison with the flow of a single equi-density spherical capsule in a horizontal HCP under same flow conditions, it has been observed that the pressure drop across a vertical HCP is 79 times higher, but as discussed above, the major contribution to this is from the elevation, rather than the presence of the capsule. In fact, it has been noticed that the contribution of capsule/s in pressure drop does not change with the elevation of the pipeline. This has been summarised in table 5.

Table 5. Pressure drop comparison, due to the capsule only, in Horizontal and Vertical HCPs

k	Vav	ΔPc (Horizontal Pipe)	ΔPc (Vertical Pipe)
0.5	1	32	31
0.5	2	114	114
0.5	3	247	245
0.5	4	429	425
0.7	1	94	94
0.7	2	340	341
0.7	3	727	729
0.7	4	1256	1254
0.9	1	1358	1378
0.9	2	4962	5028
0.9	3	10588	10833
0.9	4	18208	18447

12.7 Capsule Flow in Bends

Figure 14 depicts the static gauge pressure distribution in a horizontal bend of R/r=4 carrying a single spherical capsule of k=0.5 and having density equal to water, being transported at V_{av}=1m/sec. The results depict that the trends are similar to the one observed in a horizontal pipe, i.e. the static gauge pressure is higher at the upstream locations of the capsule. Furthermore, the pressure is less in the annulus region due to the area reduction for the flow. The pressure is recovered to some extend downstream of the capsule. The total pressure drop in this case is 169Pa, which is 36% more than for a horizontal pipe. This increase in the pressure drop is due to the generation of secondary flow features within the bend, because of its curvature.

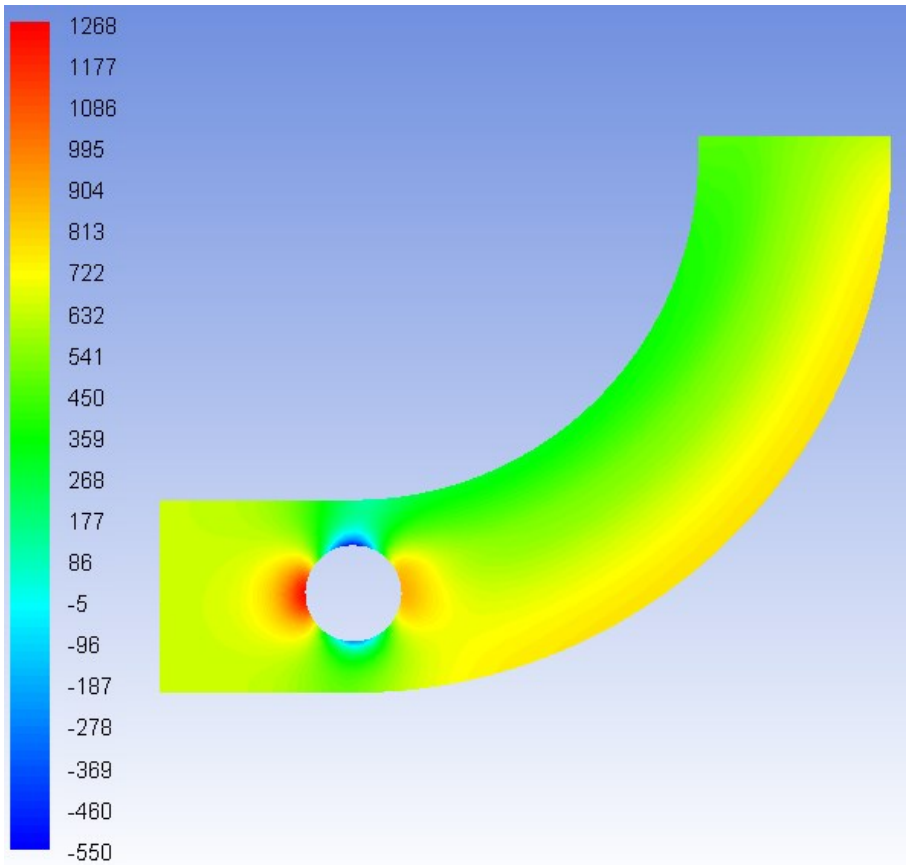

Figure 14. Variations in Static Gauge Pressure for a Single Equi-Density Spherical Capsule of k=0.5 in a Horizontal bend of R/r=4 at V_{av}=1m/sec

12.8 Effect of Bend's Curvature

Figure 15 depicts the static gauge pressure distribution in a horizontal bend of R/r=8 carrying a single spherical capsule of k=0.5 and having density equal to water, being transported at V_{av}=1m/sec. The results depict that the trends are similar to the one observed in a horizontal bend of R/r=8. The total pressure drop in this case is 151Pa, which is 10.6% lower than for R/r=4. The reason for the reduction in the pressure drop is the increase in the radius of the bend, which straightens out the bend to some extent, which decreases the magnitude of the secondary flow features within the bend. It can be thus concluded that increase in R/r of a pipe bend decreases the pressure drop across it.

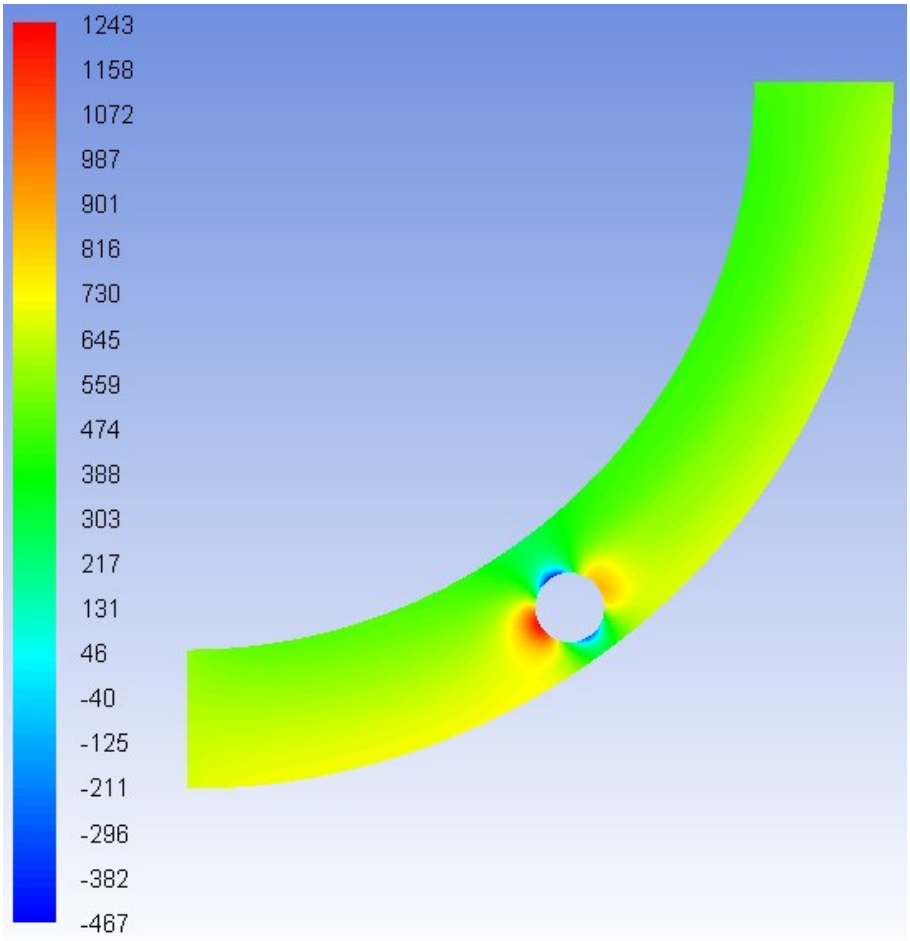

Figure 15. Variations in Static Gauge Pressure for a Single Equi-Density Spherical Capsule of k=0.5 in a Horizontal bend of R/r=8 at V_{av}=1m/sec

12.9 Novel Prediction Models for HCPs

After carrying out detailed qualitative analysis on the flow of spherical capsules in HCPs, there is a need to develop semi-empirical expressions for the capsule friction factor and loss coefficient that can be fed into the design process of an HCP using equations (5, 6, 8 and 9). However, in order to achieve this, a link between the flow parameters and the friction factor must first be established. The Darcy friction factor f on the capsules can be represented in terms of the wall shear stress acting on the capsules by:

$$f = \frac{8\tau_{wall}}{\rho {V_{av}}^2} \tag{23}$$

where τ_w is the wall shear stress. It can be seen that as the wall shear stress acting on the capsule/s increases, the friction factor increases, and in-turn pressure drop increases. Table 6 summarises the average wall shear stress acting on the surface of the capsule/s for the various HCP configurations discussed above.

Table 6. Wall Shear Stress on the Capsule/s

	Surface Average Wall Shear Stress, WSS (Pa)			Difference in WSS with respect to case 1
Case	Capsule 1	Capsule 2	Capsule 3	(%)
N/L=1, k=0.5, Vav=1m/sec	0.17	N/A	N/A	N/A
N/L=3, k=0.5, Vav=1 m/sec, Sc=1d	1.210	0.82	0.77	611.76
N/L=3, k=0.5, Vav=1 m/sec, Sc=5d	1.210	0.87	0.83	611.76
N/L=1, k=0.9, Vav=1 m/sec	12.24	N/A	N/A	7100.00
N/L=1, k=0.5, Vav=4m/sec	12.66	N/A	N/A	7347.06
N/L=1, k=0.5, Vav=1m/sec, Heavy	2.58	N/A	N/A	1417.65
N/L=1, k=0.5, Vav=1m/sec, Vertical	8.92	N/A	N/A	5147.06
k=0.5, Vav=1m/sec, R/r=4	1.34	N/A	N/A	688.24
k=0.5, Vav=1m/sec, R/r=8	1.32	N/A	N/A	676.47

It can be seen that increasing the capsule size and average flow velocity has the highest effects on the surface-average wall shear stress acting on the capsules within an HCP, followed by the inclination of the pipe and density of the capsule/s. It is however noteworthy that the spacing between the capsules has negligibly small effect on the surface-average wall shear stress acting on the front-most capsules, however, the last capsule in the train shows that the surface-average wall shear stress acting on it is 7.8% more when the spacing between the capsule increase from 1d to 5d. Furthermore, it can be seen that the surface-average wall shear stress acting on the capsules within a bend is more than in a straight pipe, and that the surface-average wall shear stress for a straighter bend (increased R/r) is less.

Both the qualitative and quantitative results shown above have been used in order to develop novel semi-empirical expressions for the capsule/s friction factor (for straight pipes) and loss-coefficient (for bends). These prediction models have been developed using advanced statistical methods such as multiple regression analysis, and represent the capsule's friction factor (and loss coefficient) as a function of non-dimensionalised parameters considered for analysis in the present study. Table 7 summarises these prediction models.

Table 7. Friction Factors for Capsules in HCPs

Pipeline Orientation	Density of the Capsules	Pipe/Bend	fc and Klc Expressions
Horizontal	Equi-Density	Pipe	$f_c = \frac{\left(2.63 \left(\frac{N}{L} * d\right)^{1.069} k^{2.56} \frac{Sc+L}{L}^{0.218}\right)}{Re_c^{0.116}}$
		Bend	$K_{lc} = \frac{\left(22387 \left(\frac{N}{L} * d\right)^{2.26} k^{3.5} \frac{Sc+L}{L}^{1.5}\right)}{Re_c^{0.38} \frac{R}{r}^{0.2}}$
	Heavy-Density	Pipe	$f_c = \frac{\left(5.25 \left(\frac{N}{L} * d\right)^{0.8} k^{4.13}\right)}{Re_c^{0.012} \frac{Sc+L}{L}^{0.164}}$
		Bend	$K_{lc} = \frac{\left(138 \left(\frac{N}{L} * d\right)^{0.66} k^{3.5}\right)}{Re_c^{0.077} \frac{R}{r}^{0.2} \frac{Sc+L}{L}^{1.17}}$
Vertical	Equi-Density	Pipe	$f_c = \frac{\left(2.75 \left(\frac{N}{L} * d\right)^{1.058} k^{2.59} \frac{Sc+L}{L}^{0.2}\right)}{Re_c^{0.12}}$
		Bend	$K_{lc} = \frac{\left(33884 \left(\frac{N}{L} * d\right)^{1.19} k^{3.24} \frac{Sc+L}{L}^{1.39}\right)}{Re_c^{0.55} \frac{R}{r}^{0.2}}$
	Heavy-Density	Pipe	$f_c = \frac{\left(5.58 \left(\frac{N}{L} * d\right)^{1.12} k^{2.64} \frac{Sc+L}{L}^{0.074}\right)}{Re_c^{0.146}}$
		Bend	$K_{lc} = \frac{\left(10^{5.6} \left(\frac{N}{L} * d\right)^{0.044} k^{4.33} \frac{Sc+L}{L}^{0.036}\right)}{Re_c^{0.83} \frac{R}{r}^{0.2}}$

where Re_c is the Reynolds number of the capsule/s, which can be expressed as:

$$Re_c = \frac{\rho_c V_c d}{\mu} \tag{24}$$

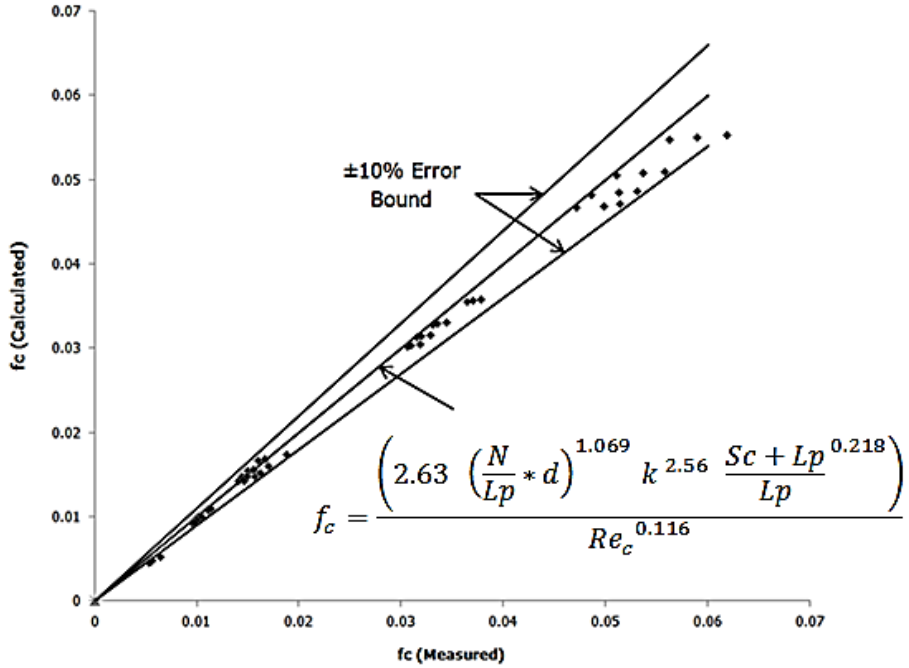

Figure 16. Difference between calculated and measured fc

All 396 numerical results have been used to develop the semi-empirical expressions of table 6. It has also been noticed that the average percentage difference between the actual results from CFD and these prediction models is ±10% for all the cases (an example shown in figure 16 above for equi-density capsules in horizontal pipe).

13. Optimisation of HCPs

Optimisation of any pipeline is essential for its commercial viability. Presented here is an optimisation model which can be used for pipelines transporting spherical capsules. The model is based on the least-cost principle, i.e. the pipeline transporting capsules is designed such that the total cost of the pipeline is minimum. The total cost of a pipeline transporting capsules consists of the manufacturing cost of the pipeline and the capsules plus the operating cost of the system.[21]

$$C_{Total} = C_{Manufacturing} + C_{Operating} \tag{25}$$

The manufacturing cost can be further divided into the cost of the pipeline and the cost of the capsules. The operating cost refers to the cost of the power being consumed.

$$C_{Total} = C_{Pipe} + C_{Capsule} + C_{Power} \tag{26}$$

13.1 Cost of Pipes

The cost of pipe per unit weight of the pipe material is given by:[39]

$$C_{Pipe} = \pi D t\, Y_p C_2 L_p \tag{27}$$

where t is the thickness of the pipe wall. According to Davis and Sorenson [40] and Russel [41], the pipe wall thickness can be expressed as:

$$t = C_c D \tag{28}$$

where C_c is a constant of proportionality dependent on expected pressure and diameter ranges of the pipeline. Hence, the cost of the pipe becomes:

$$C_{Pipe} = \pi D^2 \Upsilon_p C_2 C_c L_p \tag{29}$$

13.2 Cost of Capsules

The cost of spherical capsules per unit weight of the capsule material can be calculated as:[21]

$$C_{Spherical\ Capsules} = \pi k^2 D^2 t_c N \Upsilon_{Cap} C_3 \tag{30}$$

where t_c is the thickness of the capsule, N is the total number of capsules in the pipeline and Υ_{cap} is the specific weight of the capsule material.

13.3 Cost of Power

The cost of power consumption per unit watt is given by:[21]

$$C_{Power} = C_1 P \tag{31}$$

where P is the power requirement of the pipeline transporting capsules. It is the power that dictates the selection of the pumping unit to be installed. The power can be expressed as:

$$P = \frac{Q_m \, x \, \Delta P_{Total}}{\eta} \tag{32}$$

where Q_m is the flow rate of the mixture, ΔP_{Total} is the total pressure drop in the pipeline transporting capsules and η is the efficiency of the pumping unit. Generally the efficiency of industrial pumping unit ranges between 60 to 75%. The total pressure drop can be calculated from the friction factor (and loss-coefficient) models developed.

13.4 Mixture Flow Rate

Liu reports the expression to find the mixture flow rate as:[42]

$$Q_m = \frac{\pi D^2}{4} V_{av} \tag{33}$$

for a circular pipe.

13.5 Total Pressure Drop

The total pressure drop in a pipeline can be expressed as a sum of the major pressure drop and minor pressure drop resulting from pipeline and pipe fittings respectively.[25]

$$\Delta P_{Total} = \Delta P_{Major} + \Delta P_{Minor} \tag{34}$$

The major pressure drop can be expressed as follows for horizontal pipes as:

$$\Delta P_{Major} = f_w \frac{L}{D} \frac{\rho_w {V_{av}}^2}{2} + f_c \frac{L}{D} \frac{\rho_w {V_{av}}^2}{2} \tag{35}$$

and for vertical pipes as:

$$\Delta P_{Major} = f_w \frac{L}{D} \frac{\rho_w {V_{av}}^2}{2} + f_c \frac{L}{D} \frac{\rho_w {V_{av}}^2}{2} + \rho_w g \Delta h \tag{36}$$

Similarly, the minor pressure drop can be expressed as follows for horizontal bends as:

$$\Delta P_{Minor} = K_{lw} \frac{n\rho_w {V_{av}}^2}{2} + K_{lc} \frac{n\rho_w {V_{av}}^2}{2} \tag{37}$$

and for vertical bends as:

$$\Delta P_{Minor} = K_{lw} \frac{n\rho_w {V_{av}}^2}{2} + K_{lc} \frac{n\rho_w {V_{av}}^2}{2} + \rho_w g \Delta h \tag{38}$$

where n is the number of bends in the pipeline. Here, f_w can be found by the Moody's approximation as:[43]

$$f_w = 0.0055 + \frac{0.55}{{Re_w}^{\frac{1}{3}}} \tag{39}$$

K_{lw} has been found out to be:

$$K_{lw} = \frac{\left(3.05 - 0.0875\frac{R}{r}\right)}{{Re_w}^{\frac{1}{5}}} \tag{40}$$

13.6 Solid Throughput

The solid throughput in m^3/sec is the input to the model. One important point to note is that the pipeline designer has no information regarding the velocities in the pipeline, whether it is the average flow velocity or the velocity of the capsules. In order to replace the velocities mentioned in the above equations, the solid throughput has been used to as:

$$Solid\ Throughput = Amount\ of\ substance\ flowing\ per\ unit\ time$$

$$Q_c = Volume\ of\ a\ capsule\ x\ Time\ taken\ by\ the\ capsules\ to\ travel\ unit\ length$$

For spherical capsules:

$$Q_c = \frac{\pi d^3}{6} \; x \; \frac{Number\ of\ capsules\ in\ the\ train}{Time\ taken\ to\ travel\ unit\ length} \tag{41}$$

The number of capsules in the train can be calculated as follows:

$$L = NL_c + (N-1)S_c \tag{42}$$

where Lc is the length of the capsule/s. Hence:

$$N = \frac{L+S_c}{L_c+S_c} \tag{43}$$

where Lc=d for spherical capsules. Length of the capsules and the spacing between them should be chosen such that N is an integer. The time taken to travel unit distance will be:

$$Time\ taken\ to\ cover\ 1m\ distance\ = \ L$$

Hence:

$$Q_c = \frac{\pi d^3}{6} \; x \; \frac{L+S_c}{L_c+S_c} \; x \; \frac{V_c}{L} \tag{44}$$

$$Q_c = \frac{\pi d^3 V_c}{6L} \; x \; \frac{L+S_c}{L_c+S_c} \tag{45}$$

V_c can be represented in terms of Q_c. Furthermore, V_{av} can be expressed in terms of V_c using holdup expressions. Hence, there will be no velocity expression that will be explicitly required in the optimisation model. Figure 17 depicts the flow chart of the optimisation model developed here.

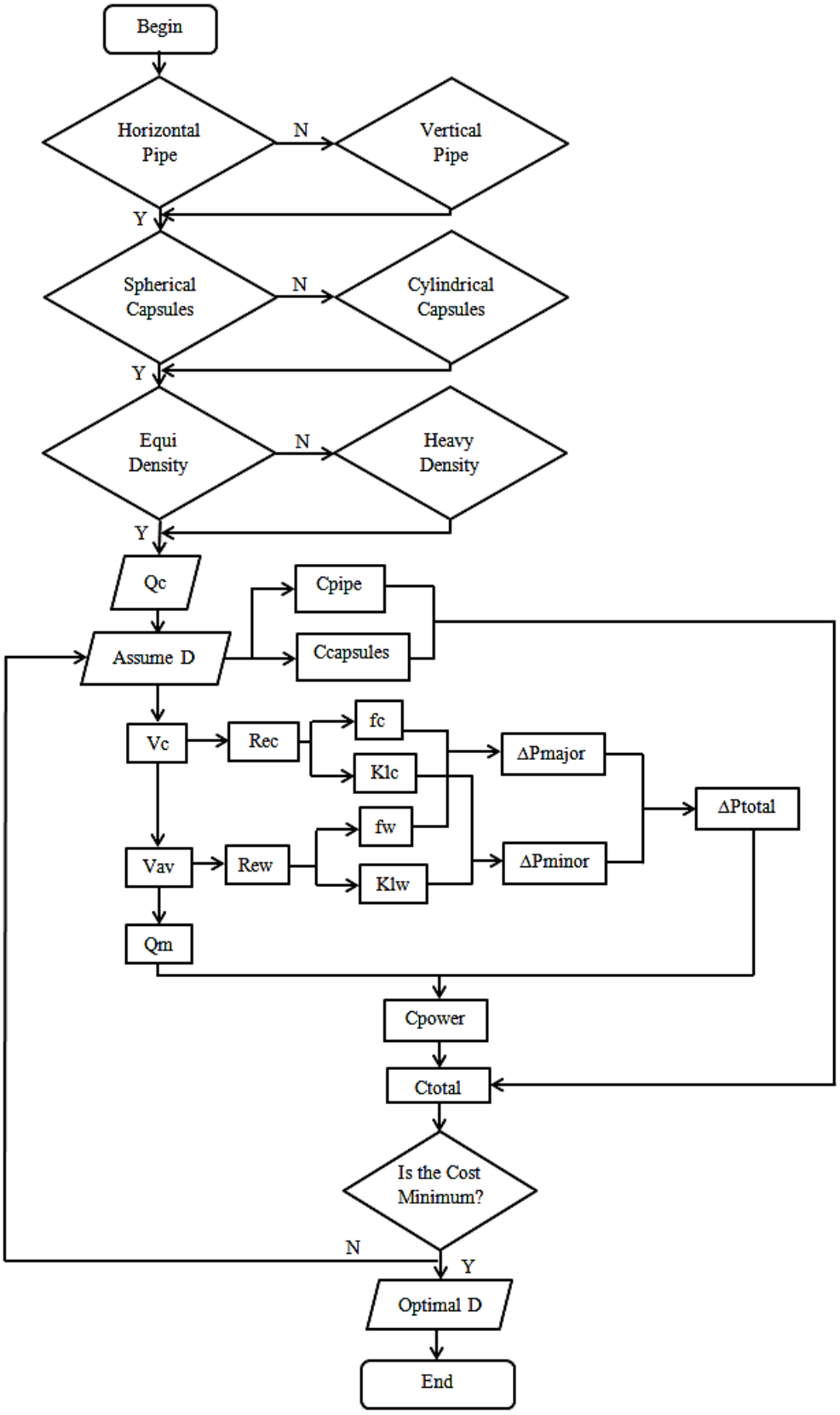

Figure 17. Flow Chart of the Optimisation Methodology

14. Design Example

Equi-density spherical capsules of k=0.7 need to be transferred from the processing plant to the storage area of the factory half kilometre away. The spacing between the capsules is 3d. The required throughput of polypropylene is 1Kg/sec. Find the optimal size of the pipeline and the pumping power required for this purpose.

Solution: According to the current market, the values of different constants involved in the optimisation process are:

$$C_1 = 1.4 \qquad C_3 = 1.1 \qquad C_2 = 0.95$$

Polypropylene has a density equal to that of water. Assuming the efficiency of the pumping unit η=60%, and following the steps described in the working of the optimisation model, the following results (table 8) are obtained. It is noteworthy that the manufacturing cost is a one-off cost, whereas the cost of power consumption is an annual cost. Hence, the total cost has one section of a one-off cost, while the other section of annual cost.

Table 8. Variations in Pumping Power and Various Costs with respect to Pipeline Diameter

D	**P**	$\mathbf{C_{Manufacturing}}$	$\mathbf{C_{Power}}$	$\mathbf{C_{Total}}$
(m)	(kW)	(£)	(£)	(£)
0.08	20.87	9129	29218	38347
0.09	11.77	11468	16487	27955
0.10	7.06	14073	9883	23956
0.11	4.44	16944	6222	23166
0.12	2.91	20081	4079	24160
0.13	1.97	23485	2766	26251
0.14	1.38	27154	1930	29084

The results presented in table 8 depicts that a pipeline of diameter=110cm is optimum for the problem under consideration because the total cost for the pipeline is minimum at D=0.11m. The power of the pumping unit required, corresponding to the optimal diameter of the pipeline, is 4.44kW. It can be further seen that as the pipeline diameter increases, the manufacturing cost increases. This is due to the fact that pipes of larger diameters are more expensive than pipes of relatively smaller diameters. Moreover, as the pipeline diameter increases, the operating cost decreases. This is due to the fact that for the same solid throughput, increasing the pipeline diameter decreases the velocity of the flow within the pipeline. The operating cost has a proportional relationship with the velocity of the flow; hence, increase in the pipeline diameter decreases the operating cost of the pipeline.

16. Conclusions

From detailed numerical investigations, it has been found out that the presence of spherical capsule/s within a hydraulic pipeline increases the resistance to the flow within such pipelines, hence increasing the pressure drop. It has been observed that the static gauge pressure within an HCP varies significantly based on the capsule concentration, size, density, flow velocity, pipe's inclination etc. Increase in capsule concentration increases the pressure drop, while the spacing between the capsules has negligibly small effect on it. Increase in capsule size increases the pressure drop across the pipeline, however, increasing the capsule size from k=0.5 to 0.7 results in lesser pressure drop increment as compared to increasing the capsule size from k=0.7 to 0.9. Heavier spherical capsules offer more resistance to the flow because of non-uniform static gauge pressure variations in the HCPs. Similarly, increasing the average flow velocity increases the pressure drop across the pipeline.

It has also been observed that although the pressure drop across a vertical HCP is considerably higher as compared to a horizontal HCP, however, the resistance offered by the capsule/s is almost the same, and the main difference in the pressure drop arises from the elevation of the pipe. Furthermore, it has been noticed that pressure drop across pipe bends is higher as compared to a straight pipeline, and hence, straightening a bend (by increasing its R/r) offers lower pressure drop across the pipe bend. Based on these results, novel semi-empirical prediction models have been developed for the friction factor of capsules, which have been used in an optimisation model developed based on least-cost principle. The optimisation model's sole input is the solid throughput required from the HCP, while the main output is the optimal pipeline diameter. A practical example has been included in order to demonstrate the usage and effectiveness of this optimisation model.

References

[1] H. Liu, (1992) "Hydraulic Behaviours of Coal Log Flow in Pipe", In the Proceedings of the 4th International Conference on Bulk Materials Handling and Transportation; Symposium on Fright Pipelines, Wollongong, Australia

[2] Barthes-Biesel, D. (2009) "Capsule motion in flow: Deformation and Membrane Buckling", C. R. Physique, vol: 10, pp: 764 – 774

[3] Barthes-Biesel, D. (2011) "Modelling the motion of Capsules in Flow", Journal of Colloid & Interface Science, vol: 16, pp: 3 – 12

[4] Rachik, M. Barthes-Biesel, D. Carin, M. Edwards-Levy, F. (2006) "Identification of the elastic properties of an artificial capsule membrane with the compression test: Effect of thickness", Journal of Colloid & Interface Science, vol: 301, pp: 217 – 226

[5] Subramanya, K. (1998) "Pipeline transportation technology: An overview", Current Science, vol. 75, pp. 824

[6] Ellis, H. S. (1964) "An Experimental Investigation of the Transport by Water of Single Cylindrical and Spherical Capsules with Density Equal to that of the Water", The Canadian Journal of Chemical Engineering, vol: 42, Issue: 1, pp: 1 – 8

[7] Ellis, H. S. (1964) “An Experimental Investigation of the Transport by Water of Single Spherical Capsules with Density Greater than that of the Water”, The Canadian Journal of Chemical Engineering, pp. 155 – 160

[8] Ellis, H. S. Kruyer, J. Roehl, A. A. (1975) “The Hydrodynamics of Spherical Capsules”, The Canadian Journal of Chemical Engineering, vol. 53, pp. 119 – 125

[9] Mathur, R. Rao, C. R. Agarwal, V. C. (1989) “Transport Velocity of Equal Density Spherical Capsules in Pipeline”, In the Proceedings of the 4th Asian Congress of Fluid Mechanics, Hongkong, pp: 106 – 109

[10] Round, G. F. Bolt, L. H. (1965) “An Experimental Investigation of the Transport in Oil of Single, Denser-than Oil, Spherical and Cylindrical Capsules”, The Canadian Journal of Chemical Engineering, pp: 197 – 205

[11] Mishra, R. Agarwal, V. C. Mathur, R. (1992) “Empirical Relations for Spherical Capsules of Various Densities”, In the Proceedings of the 19th National Conference on Fluid Mechanics and Fluid Power, Bombay

[12] Newton, R. Redberger, P. J. Round, G. F. (1963) “Numerical Analysis of Some Variables Determining Free Flow”, The Canadian Journal of Chemical Engineering, vol: 42, Issue: 4, pp: 168 – 173

[13] Ulusarslan, D. Teke, I. (2006) “An Experimental Determination of Pressure Drops in the Flow of Low Density Spherical Capsule Train Inside Horizontal Pipes, Journal of Experimental Thermal and Fluid Science, vol: 30, pp: 233 – 241

[14] Chow, K. W. (1979) “An Experimental Study of the Hydrodynamic Transport of Spherical and Cylindrical Capsules in a Vertical Pipeline”, M. Eng. Thesis, McMaster University, Hamilton, Ontario, Canada

[15] Latto, B. Chow, K. W. (1982) “Hydrodynamic Transport of Cylindrical Capsules in a Vertical Pipeline”, The Canadian Journal of Chemical Engineering, vol. 60, pp. 713 – 722

[16] Ulusarslan, D. (2007) “Determination of the Loss Coefficient of Elbows in the Flow of Low-Density Spherical Capsule Train”, Experimental Thermal and Fluid Science, vol. 32, pp. 415 – 422

[17] Polderman, H. G. (1982) “Design Rules for Hydraulic Capsule Transport Systems”, Journal of Pipelines, vol. 3, pp. 123 – 136

[18] Assadollahbaik, M. Liu, H. (1986) “Optimum Design of Electromagnetic Pump for Capsule Pipelines”, Journal of Pipelines, vol. 5, pp. 157 – 169

[19] Swamee, P. K. (1995) “Design of Sediment Transporting Pipeline”, Journal of Hydraulic Engineering, vol. 121

[20] Swamee, P. K. (1999) “Capsule Hoist System for Vertical Transport of Minerals”, Journal of Transportation Engineering, pp. 560 – 563

[21] Agarwal, V. C. Mishra, R. (1998) “Optimal Design of a Multi-Stage Capsule Handling Multi-Phase Pipeline”, International Journal of Pressure Vessels and Piping, vol. 75, pp. 27 – 35

[22] Colebrook, C.F. (1939) “Turbulent Flow in Pipes with Particular Reference to the Transition Region between Smooth and Rough Pipe Laws” Journal of the Institution of Civil Engineers

[23] Sha, Y. Zhao, X. (2010) “Optimisation Design of the Hydraulic Pipeline Based on the Principle of Saving Energy Resources”, In the Proceedings of Power and Energy Engineering Conference, Asia-Pacific

[24] Darcy, H. (1857) “Recherches Expérimentales Relatives au Mouvement de l’Eau dans les Tuyaux [Experimental Research on the Movement of Water in Pipes]”, Mallet-Bachelier, Paris

[25] Munson, B. R. Young, D. F. Okiishi, T. H. (2002) “Fundamentals of Fluid Mechanics”, John Willey & Sons Inc., 4th ed., U.S.A., ISBN: 0471675822

[26] Ulusarslan, D. Teke, I. (2005) “An Experimental Investigation of the Capsule Velocity, Concentration Rate and the Spacing between the Capsules for the Spherical Capsule Train Flow in a Horizontal Circular Pipe”, Journal of Powder Technology, vol: 159, pp: 27 – 34

[27] Industrial Accessories Company accessible at http://www.iac-intl.com/parts/PB103001r2.pdf

[28] Morsi, S. A. Alexander, A. J. (1972) “An Investigation of Particle Trajectories in Two-Phase Flow Systems”, Journal of Fluid Mechanics, vol. 55, pp. 193 – 208

[29] Stone, H. A. (2000) “Philip Saffman and Viscous Flow Theory”,Journal of Fluid Mechanics, vol. 409, pp:165 – 183

[30] Khalil, M. F. Kassab, S. Z. Adam, I. G. Samaha, M. A. (2009) “Prediction of Lift and Drag Coefficients on Stationary Capsule in Pipeline”, CFD Letters, vol. 1, pp: 15 – 28

[31] Patankar, S. V. Spalding, D. B. (1972), “A Calculation Procedure for Heat, Mass and Momentum Transfer in Three-Dimensional Parabolic Flows”, Heat and Mass Transfer, vol. 15, pp: 1787 – 1806

[32] Rauch, R. D. Batira, J. T. Yang, N. T. Y. (1991) “Spatial Adaption Procedures on Unstructured Meshes for Accurate Unsteady Aerodynamic Flow Computations”, Technical Report, American Institute of Aeronautics and Astronautics, vol. 91, pp: 1106

[33] Barth, T. J. Jespersen, D. (1989) "The Design and Application of Upwind Schemes on Unstructured Meshes", 27th Technical Report, Aerospace Sciences Meeting, Nevada

[34] Ulusarslan, D. Teke. I. (2009) "Relation between the Friction Coefficient and Re Number for Spherical Capsule Train-Water Flow in Horizontal Pipes", Particulate Science and Technology, vol: 27, pp: 488 – 495

[35] Ulusarslan, D. (2009) "Effect of Capsule Density and Concentration on Pressure Drops of Spherical Capsule Train Conveyed by Water", Journal of Fluids Engineering, vol: 132

[36] Ariyaratne, C. (2005) "Design and Optimisation of Swirl Pipes and Transition Geometries for Slurry Transport", Ph.D. Thesis, The University of Nottingham

[37] Uluasarslan, D. (2008) "Comparison of Experimental Pressure Gradient and Experimental Relationships for the Low Density Spherical Capsule Train with Slurry Flow Relationships", Powder Technology, vol. 185, pp: 170 – 175

[38] Teke, I. Uluasarslan, D. (2007) "Mathematical Expression of Pressure Gradient in the Flow of Spherical Capsules Less Dense than Water", International Journal of Multiphase Flow, vol. 33, pp: 658 – 674

[39] Cheremisinoff, P. N. Cheng, S. I. (1988) "Civil Engineering Practice", Technomies Publishing Co., Lancaster, P. A., U.S.A., ISBN: 0877625409

[40] Davis, C. Sorensen, K. (1969) "Handbook of Applied Hydraulics", McGraw-Hill Book Co., New York, 3rd ed., U.S.A., ISBN: 0070730024

[41] Russel, G. (1963) "Hydraulics", Holt, Rinehart and Winston, New York, 5th ed., U.S.A., EAN: BWB12771249

[42] Liu, H. (2005) "Pipeline Engineering", Lewis Publishers, New York, U.S.A., ISBN: 978-1587161407

[43] Moody, L. F. (1944) "Friction factors for pipe flow", Transactions of the ASME, vol. 66, pp. 671– 684

NOMENCLATURE

A	Cross-sectional Area of the Pipe (m^2)
C_1	Cost of Power consumption per unit Watt (£/W)
C_2	Cost of Pipe per unit Weight of Pipe material (£/N)
C_3	Cost of Capsules per unit Weight of the Capsule Material (£/N)
C_c	Constant of Proportionality
C_D	Drag Coefficient
c	Concentration of Solid Phase
d	Diameter of Capsule/s (m)
D	Diameter of Pipe (m)
F_D	Drag Force (N)
f	Darcy Friction Factor
g	Acceleration due to gravity (m/sec^2)
h	Elevation (m)
H	Holdup Velocity
k	Capsule to Pipe diameter ratio
K_l	Loss Coefficient of Bends
L	Length (m)
n	Number of Bends
N	Number of Capsules
ΔP	Pressure Drop (Pa)
Q	Flow Rate (m^3/sec)
R	Radius of Curvature of Pipe Bend (m)
r	Radius of Pipe (m)

Re	Reynolds Number
s	Specific Gravity
Sc	Spacing between the Capsules (m)
t	Time (sec)
u_*	Friction Velocity at the nearest wall (m/sec)
V	Flow Velocity (m/sec)
y	Nearest Wall Distance (m)
y^+	Non-dimensional Wall Distance

SYMBOLS

ρ	Density (Kg/m^3)
μ	Dynamic Viscosity (Pa-sec)
ε	Roughness Height of the Pipe (m)
Υ	Specific Weight (N/m^3)
η	Efficiency of the Pump (%)
θ	Inclination Angle of Pipe (^{o})
π	Pi
τ_{Wall}	Wall Shear Stress (Pa)

SUBSCRIPTS

av	Average
c	Capsule
m	Mixture
p	Particle
w	Water

Vitae

Taimoor Asim holds his Ph.D. in the area of Computational Fluid Dynamics based design of Hydraulic Capsule Pipelines from the University of Huddersfield (UK). He is currently a Research Fellow in Flow Diagnostics at the University of Huddersfield. His areas of interest are Computational Fluid Dynamics, Multi-phase flows, Pipeline Engineering and Hydrodynamics. He has published more than 30 papers in various journals and conference proceedings.

Rakesh Mishra is currently a Professor of Fluid Dynamics at the University of Huddersfield, UK. He heads the Energy Emissions and the Environment research group within the Diagnostics research centre at the University of Huddersfield. He has published more than 150 papers in various journals and conference proceedings.